mathematics

MDPI

Article

Influence of Bioconvection and Chemical Reaction on Magneto—Carreau Nanofluid Flow through an Inclined Cylinder

Hossam A. Nabwey [1,2,*], Sumayyah I. Alshber [3], Ahmed M. Rashad [4] and Abd El Nasser Mahdy [5]

[1] Department of Mathematics, College of Science and Humanities in Al-Kharj, Prince Sattam bin Abdulaziz University, Al-Kharj 11942, Saudi Arabia
[2] Department of Basic Engineering Science, Faculty of Engineering, Menoufia University, Shebin El-Kom 32511, Egypt
[3] Department of Mathematics, College of Education in Al-Dilam, Prince Sattam bin Abdulaziz University, Al-Kharj 11942, Saudi Arabia; s.alshabr@psau.edu.sa
[4] Department of Mathematics, Faculty of Science, Aswan University, Aswan 81528, Egypt; am_rashad@yahoo.com
[5] Mathematics Department, Faculty of Science, South Valley University, Qena 83523, Egypt; mahdy4@yahoo.com
* Correspondence: eng_hossam21@yahoo.com

Abstract: The present contribution focuses on heat transmission in the conjugate mixed bioconvection flow of Carreau nanofluid with swimming gyrotactic microorganisms through an inclined stretchable cylinder with variable magnetic field impact and binary chemical reaction. Additionally, the investigation involves the aspects of variable decrease or increase in heat source and non-uniform thermal conductivity. A passively controlled nanofluid pattern is used to estimate this nano-bioconvection flow case, which is believed to be more physically accurate than the earlier actively controlled nanofluid typically employed. One of essential features of this investigation is the imposition of a zero-mass flux condition at the surface of the cylinder. Through the implementation of an appropriate transformation, the nonlinear PDE system is mutated into similar equations. The flow equations thus obtained are solved numerically to explore the influence of the physical constraints involved through implementation with the aid of the MATLAB bvp4c code. The solutions were captured for both zero and non-zero bioconvection Rayleigh number, i.e., for flow with and without microorganisms. The present numerical results are compared with the available data and are determined to be in excellent agreement. The significant result of the present article is that the degree of nanoparticle concentration in the nanofluid exhibits an increasing trend with higher values of activation energy constraint.

Keywords: Carreau nanofluid; bioconvection; non-uniform thermal conductivity; microorganisms; binary chemical reaction; cylinder

check for updates

Citation: Nabwey, H.A.; Alshber, S.I.; Rashad, A.M.; Mahdy, A.E.N. Influence of Bioconvection and Chemical Reaction on Magneto—Carreau Nanofluid Flow through an Inclined Cylinder. *Mathematics* **2022**, *10*, 504. https://doi.org/10.3390/math10030504

Academic Editor: Efstratios Tzirtzilakis

Received: 7 January 2022
Accepted: 3 February 2022
Published: 4 February 2022

1. Introduction

Newtonian liquids can be entirely elaborated on the basis of the impacts of pressure and temperature, but the physical aspects of non-Newtonian liquids also take into account the effects of the forces acting on them over time. The viscosity of miscellaneous liquids does not depend on the imposed (shearing) force. In any case, there is a specific set of fluids that exhibit an essentially different behavior. One of the categories of these miscellaneous liquids is shear-thinning, in which the (apparent) viscosity is inversely proportional to the strain rate. The constitutive pattern presented by Carreau [1] includes four additional factors compared to Newtonian fluids; therefore, it is able to describe the rheology of a vast range of non-Newtonian liquids. This pattern fits reasonably well in miscellaneous flow situations, in particular, for some dilute, aqueous, and polymer solutions, as well as melts. Chhabra and Uhlherr [2] presented the earliest theoretical investigation of the creeping flow of the non-Newtonian Carreau liquid caused by a sphere. Laminar and

double diffusion flow within a heated cavity containing Carreau fluid was simulated by Tang and Kefayati [3]. Sochi [4] provided analytical formulas associating the volumetric flow rate with the pressure drop, deduced for the flow of Carreau and Cross liquids over thin slits and uniform circular tubes. The problem presented by the Von-Karman infinite disk in relation to non-Newtonian liquids was addressed by Griffiths [5], who implemented the Carreau pattern. Griffiths determined that that the Carreau viscosity pattern did not suffer under any non-physical situations that could be encountered when dealing with power-law patterns. Liron and Wilhelm [6] investigated the attitude of viscous liquid when incorporating the impact of a magnetic field in a transverse trend with respect to the flow. Soomro et al. [7] analyzed the MHD mixed convective flow pattern with thermal velocity slip impacts. The MHD free and forced convection fluid flow was examined by Pal et al. [8], evaluating the impact of thermal radiation on a stretching and shrinking surface geometry. Daniel et al. [9] obtained mixed convection flow in an electrically conductive nanoliquid as a result of magnetohydrodynamics. Shankaralingappa [10,11] presented a numerical analysis of the thermal and mass distribution of a 3-D non-linear extending plate with Al_2O_3-based non-Newtonian nanoliquid with thermophoretic particle deposition and relaxation chemical reaction. In this context, a number of fruitful research papers that are related to the current contribution have been published by several authors [12–18].

In addition, bioconvection refers to an attractive phenomenon in fluid mechanics that has a variety of applications in bioscience and life science technology. The theory of bioconvection explores impulsive pattern construction and mass stratification with respect to the immediate communication among microbes, forces, and nanoparticles. The bioconvective flow of non-Newtonioan Sisko nanofluid was scrutinized with respect to activation energy and gyrotactic microorganisms by Khan et al. [19], while Waqas et al. [20] considered non-Newtonian second-grade nanofluid. Shen et al. [21] considered a stretching sheet in order to examine the heat transference in a bioconvective fluid flow containing nanomaterials and gyrotactic microorganisms. Balla et al. [22] presented a case of bioconvective nanofluid flow in a porous medium consisting of nanoparticles and oxytactic microbes. Several contributions related to bioconvection have been published focusing on the suspension of gyrotactic/oxytactic microorganisms in a variety of scenarios [23–33]. Furthermore, materials possessing a magnitude of 1 nm to 100 nm are denominated as being nanoparticles or nanomaterials. The use of these kinds of nanoparticles was first undertaken by Choi [34], who used these nanoparticles within a pure liquid, popularizing the denotation of such a mixture as a nanofluid. The denotation as nanoliquids was first described by Buongiorno [35], who introduced a two-phase pattern known as the Buongiorno two-phase model. Using this model, he inspected the features of nanoliquids by employing both thermophoresis and Brownian diffusion processes. Since then, a number of researchers have made contributions in the field of nanoliquids, as nanoliquids have magnificent thermophysical features. Tunde et al. [36] elucidated the entropy generation in the bioconvective flow of Williamson nanoliquid through an oblique semi-infinite surface immersed in porous media under the impact of gyrotactic microorganisms and thermal radiation.

Activation energy describes the lowest amount of energy needed to instigate a chemical reaction inside the system. In a small number of cases, it can be observed that the activation energy is equal to zero. The instigation of a chemical reaction in order to examine activation energy is necessary due to its enormous applications in chemical engineering, mechanical chemistry, and the cooling of nuclear reactors. This sort of energy has been investigated by several authors in their papers. Majeed et al. [37] reported Arrhenius activation energy for the Darcy-Forchheimer flow case with a fluid with an external magnetic field past a stretchable sheet, focusing on the chemical reaction and the second-order slip effect. The influence of both the activation energy and the chemical reaction of MHD mixed convectional stagnation point via a stretching plate of Cross nanoliquid was examined by Khan et al. [38]. Mustafa et al. [39] numerically analyzed the effects of the activation energy of an MHD mixed convective flow of nanoliquid over a vertical stretching surface.

Dhlamini et al. [40] investigated the trends of activation energy and the binary chemical reaction in a time-dependent flow of mixed convective nanoliquid. Shafique et al. [41] proposed a mathematical pattern for analyzing the combined impacts of heat and mass transmission of Maxwell liquid flow with a binary chemical reaction produced by activation energy. Additionally, since magnetohydrodynamics (MHD) has a wide range of applications, e.g., petroleum, environmental, and chemical technologies, it has attracted a great deal of attention. The expression MHD denotes the employment of a magnetic field, often imposed normal to the trend of liquid flow, which has the potential to impose a drag force, referred to as the Lorentz force. The generated force acts against the trend of the liquid flow, in turn impacting the fluid motion. Zhao et al. [42] discussed the aspect of magnetic field heat transmission of nanoliquids in microchannels. Waqas et al. [43] addressed MHD free and forced convection flow of non-Newtonian liquid through a nonlinear stretching surface.

Inspired by the abovementioned literature and applications, the aim of the current paper is to analyze the impact of the activation energy and mixed bioconvection flow of Carreau nanofluid including gyrotactic microorganisms past an oblique slender cylinder. The imposed thermal conductivity and magnetic field are varied. The mathematical pattern is based on a system of nonlinear differential equations under boundary layer assumptions. The viable similarity conversion technique reduces the modeled flow equations to an ODE set which is then solved numerically with the assistance of the MATLAB bvp4c code. The influence of a variety of involved factors and physical quantities is determined numerically and presented graphically. To the best of our knowledge, this problem has not yet been considered.

2. Flow Analysis

Let us configure a time-dependent magnetohydrodynamic (MHD) mixed bioconvection flow resulting from swimming gyrotactic microorganisms for a Carreau nanoliquid through an oblique permeable stretched cylinder at an angle Ω with the horizontal axis, as portrayed in Figure 1. The cylinder is stretched with a linear stretching velocity $U_w = \frac{ax}{1-\zeta t}$. Furthermore, the conditions of non-uniform thermal conductivity and zero-mass flux are imposed on the cylinder surface. A variable magnetic field is employed in such a way that the cylinder is perpendicular to it and the Carreau nanofluid is presumed to be electrically conducting with an intensity $B(t) = \frac{B_0}{(1-\zeta t)^{1/2}}$, where B_0 represents a constant. The surface of the permeable cylinder is kept at a constant temperature T_w with a constant density of motile microorganisms N_w, whereas far from the cylinder surface, the temperature, the nanoparticle volume fraction, and the concentration of microorganisms are given as T_∞, C_∞ and N_∞, respectively. The constitutive equation for the Carreau rheological pattern [18] can be formulated as

$$\mu = \mu_\infty + (\mu_0 - \mu_\infty)\left(1 + (\tilde{\gamma}\dot{\gamma})^2\right)^{\frac{n-1}{2}} \tag{1}$$

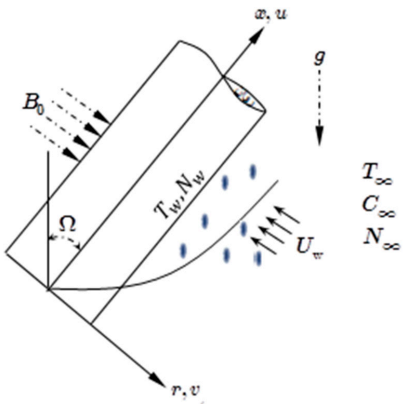

Figure 1. Physical configuration of the problem.

Herein, μ_∞, μ_0, $\widetilde{\gamma}$ and n represent the viscosities at infinite and zero shear rate, the material constant, and the power-law index. For the value of n, when (n = 1), the fluid is described as possessing a Newtonian attitude, (0 < n < 1) represents the shear-thinning attitude, and (n > 1) represents a shear-thickening fluid. Here, the state equation at infinite shear rate viscosity ($\mu_\infty = 0$) is recognized. Therefore, the constitutive Equation (2) is re-expressed as $\mu = \mu_0\left(1 + (\widetilde{\gamma}\dot{\gamma})^2\right)^{(n-2)/2}$. The shear rate $\dot{\gamma}$ is formulated as $\dot{\gamma} = \sqrt{0.5 \text{ tr } A_1^2}$, in which $A_1 = \nabla \mathrm{V} + (\nabla \mathrm{V})^T$ is the 1st Rivlin–Erickson tensor, with V being the velocity. Furthermore, the thermal conductivity of the Carreau liquid can be expressed by the following relation [44]:

$$k_f = k_\infty\left(1 + \epsilon\frac{T - T_\infty}{T_\mathrm{w} - T_\infty}\right)$$

where ϵ denotes the non-uniform thermal conductivity factor, and k_∞ stands for the ambient thermal conductivity of the Carreau nanoliquid. The impact of the binary chemical reaction is imposed in order to determine the sloutal energy transport behavior of the Carreau nanofluid. On the basis of these hypotheses, the 2-D fundamental flow formulas employed are those given by [14,17,41].

$$\frac{\partial(ru)}{\partial x} + \frac{\partial(rv)}{\partial r} = 0 \tag{2}$$

$$\begin{gathered}\frac{\partial u}{\partial t} + u\frac{\partial u}{\partial x} + v\frac{\partial u}{\partial r} = \nu_f\left(1 + \widetilde{\gamma}^2\left(\frac{\partial u}{\partial r}\right)^2\right)^{\frac{n-1}{2}}\left(\frac{1}{r}\frac{\partial u}{\partial r} + \frac{\partial^2 u}{\partial r^2}\right) - \frac{\sigma B_0^2}{\rho_f}u \\ +\frac{g}{\rho_f}\left(\rho_f\beta_f(1-C_\infty)(T-T_\infty) - \left(\rho_p - \rho_f\right)(C-C_\infty) - \gamma^\star\left(\rho_m - \rho_f\right)(N-N_\infty)\right)\cos\Omega \\ +(n-1)\nu_f\widetilde{\gamma}^2\left(\frac{\partial u}{\partial r}\right)^2\frac{\partial^2 u}{\partial r^2}\left(1 + \widetilde{\gamma}^2\left(\frac{\partial u}{\partial r}\right)^2\right)^{\frac{n-3}{2}}\end{gathered} \tag{3}$$

$$\frac{\partial T}{\partial t} + u\frac{\partial T}{\partial x} + v\frac{\partial T}{\partial r} = \frac{1}{(\rho c_\mathrm{p})_f}\frac{1}{r}\left(\frac{\partial}{\partial r}\left(k_f\frac{\partial T}{\partial r}\right)\right) + \jmath\left(D\frac{\partial T}{\partial r}\frac{\partial C}{\partial r} + \frac{\overline{D}}{T_\infty}\left(\frac{\partial T}{\partial r}\right)^2\right) \tag{4}$$

$$\frac{\partial C}{\partial t} + u\frac{\partial C}{\partial x} + v\frac{\partial C}{\partial r} = \frac{D}{r}\frac{\partial}{\partial r}\left(r\frac{\partial C}{\partial r}\right) + \frac{\overline{D}}{T_\infty}\frac{1}{r}\frac{\partial}{\partial r}\left(r\frac{\partial T}{\partial r}\right) - k_\mathrm{r}^2(C - C_\infty)\left(\frac{T}{T_\infty}\right)^m \mathrm{e}^{-\left(\frac{E_0}{k^\star T}\right)} \tag{5}$$

$$\frac{\partial N}{\partial t} + u\frac{\partial N}{\partial x} + v\frac{\partial N}{\partial r} + \frac{bW_\mathrm{c}}{C_\infty}\frac{1}{r}\frac{\partial}{\partial r}\left(rN\frac{\partial C}{\partial r}\right) = \frac{\widetilde{D}}{r}\frac{\partial}{\partial r}\left(r\frac{\partial N}{\partial r}\right) \tag{6}$$

On the basis of the controlling flow equation, x and r are Cartesian coordinates, (u, v) indicate the velocity components of the Carreau two-phase nanofluid along the x- and r-axes, respectively, T, C stand for the nanofluid temperature and concentration, N gives the micro-rotation velocity, the gravity acceleration is indicated by g, $\gamma^\star$ denotes the average volume of the microorganisms, k_f, k_r denote the nanofluid thermal conductivity and chemical reaction constant, W_c is a constant representing the maximum cell swimming speed, ρ_p is the density of the nanoparticles, D, $\overline{D}$, $\widetilde{D}$ are the Brownian and thermophoretic diffusions and diffusivity of microorganisms, respectively, and the density of the motile microorganism is indicated by ρ_m. Additionally, realistic flow boundary conditions for the Carreau nanofluid are imposed as stated as [17,25]:

$$\begin{gathered}u = U_\mathrm{w},\ v = 0,\ T = T_\mathrm{w}\ D\frac{\partial C}{\partial r} + \frac{\overline{D}}{T_\infty}\frac{\partial T}{\partial r} = 0,\ N = N_\mathrm{w} \text{at } r = R \\ u \to 0,\ T \to T_\infty,\ C \to C_\infty,\ N \to N_\infty, \text{as } r \to \infty\end{gathered} \tag{7}$$

Let us mutate the above flow equations into dimensionless form using the following transformation [17,36]:

$$\begin{gathered}\eta = \frac{r^2 - R^2}{2R}\left(\frac{a}{\nu_f(1-\zeta t)}\right)^{1/2},\ \psi = \left(\frac{a\nu_f}{1-\zeta t}\right)^{1/2} xRF(\eta), \\ \theta(\eta) = \frac{T - T_\infty}{T_\mathrm{w} - T_\infty},\ \phi(\eta) = \frac{C - C_\infty}{C_\infty},\ \vartheta(\eta) = \frac{N - N_\infty}{N_\mathrm{w} - N_\infty}\end{gathered} \tag{8}$$

Herein, $u = \frac{1}{r}\frac{\partial\psi}{\partial r}$ and $v = -\frac{1}{r}\frac{\partial\psi}{\partial x}$. Of course, the continuity equation (Equation (1)) is obtained automatically, and other equations of flow turn into

$$\begin{gathered}(1+2\gamma\eta)(1+W_eF''^2)^{\frac{n-3}{2}}\left(1+n\ W_eF''^2\right)F''' + \gamma(1+W_eF''^2)^{\frac{n-3}{2}}\left(2+(n+1)W_eF''^2\right)F'' \\ +FF'' - F'^2 - A\left(\tfrac{1}{2}\ \eta F'' + F'\right) - M\ F' + R_i(\theta - N_r\ \phi - R_b\vartheta)\cos\Omega = 0\end{gathered} \tag{9}$$

$$\begin{gathered}(1+2\gamma\eta)\left((1+\epsilon\theta)\theta'' + \epsilon\theta'^2\right) + 2\gamma\theta\prime(1+\epsilon\theta) + \mathrm{Pr}F\theta' - \tfrac{1}{2}A\ \mathrm{Pr}\ \eta\ \theta' \\ +\mathrm{Pr}(1+2\gamma\eta)\left(Nb\theta'\phi' + Nt\theta'^2\right) = 0\end{gathered} \tag{10}$$

$$\begin{gathered}(1+2\gamma\eta)\phi'' + \left(2\gamma - \tfrac{1}{2}A\ L_e\ \eta\right)\phi' + L_eF\phi' + \tfrac{N_t}{N_b}(2\gamma\theta' + (1+2\gamma\eta)\theta'') \\ -L_eK_{\mathrm{r}}\phi(\delta\theta+1)^m\mathrm{e}^{-\frac{E}{\delta\theta+1}} = 0\end{gathered} \tag{11}$$

$$\begin{gathered}(1+2\gamma\eta)\vartheta'' + \left(2\gamma - \tfrac{1}{2}A\ L_b\ \eta\right)\vartheta' + L_b\ F\vartheta' \\ -P_{\mathrm{e}}(\vartheta+\omega)(1+2\gamma\eta)(\phi'' + 2\gamma\phi') - P_{\mathrm{e}}(1+2\gamma\eta)\phi'\vartheta' = 0\end{gathered} \tag{12}$$

With the newly transformed flow boundary conditions

$$\begin{gathered}F' = 1,\ F = 0,\ \theta = 1,\ N_b\phi' + N_t\theta' = 0\ \vartheta = 1,\ \text{when}\ \eta = 0 \\ F' \to 0,\ \theta \to 0,\ \phi \to 0,\ \vartheta \to 0,\ \text{when}\ \eta \to \infty\end{gathered} \tag{13}$$

The parameters appearing in the mutated governing equations can be defined as follows: $W_{\mathrm{e}} = \frac{a^3x^2r^2\widetilde{\gamma}^2}{(1-\zeta t)^3R^2\nu_f}$ stands for Weissenberg number, $\gamma = \left(\frac{(1-\zeta t)\nu_f}{aR^2}\right)^{1/2}$ is the curvature parameter, $M = \frac{\sigma B_0^2}{a\rho_f}$ is the magnetic field factor, $R_i = \frac{g\beta_f(1-C_\infty)(T_{\mathrm{w}}-T_\infty)x}{U_{\mathrm{w}}^2}$ refers to the mixed convection factor, $N_t = \frac{J\overline{D}(T_{\mathrm{w}}-T_\infty)}{\nu_f T_\infty}$ gives the thermophoresis diffusion factor, $N_b = \frac{JDC_\infty}{\nu_f}$ indicates the Brownian diffusion factor, $N_r = \frac{(\rho_p - rho_f)C_\infty}{\beta_f\rho_f(1-C_\infty)(T_{\mathrm{w}}-T_\infty)}$ denotes the buoyancy force ratio factor, $\mathrm{Pr} = \frac{\mu c_p}{k_f}$ represents the Parndtl number, $L_e = \frac{\nu_f}{\widetilde{D}}$ is the Lewis number, $R_b = \frac{\gamma^\star(\rho_p-\rho_f)}{\beta_f\rho_f(1-C_\infty)(T_{\mathrm{w}}-T_\infty)}$ denotes the bioconvection Rayleigh number, $L_b = \frac{\nu_f}{\widetilde{D}}$ refers to the bioconvection Lewis number, $A = \frac{\zeta}{a}$ is the unsteadiness parameter, $P_e = \frac{bW_{\mathrm{c}}}{\widetilde{D}}$ indicates the Peclet number, $K_{\mathrm{r}} = \frac{k_r^2}{a}$ is the chemical reaction factor, $E = \frac{E_0}{k^\star T_\infty}$ gives the activation energy factor, $\delta = \frac{E_0}{k^\star T_\infty}$ is the temperature difference factor, and $\omega = \frac{N_\infty}{N_{\mathrm{w}}-N_\infty}$ denotes the microorganism concentration difference factor.

On the basis of the dimensionless variables, the significant physical quantities in the design—the skin friction factor C_f, the Nusselt number Nu, and the density of the motile microorganisms Nn—can be given in the following form:

$$C_f = \frac{\tau_w|_{r=R}}{\rho_f U_w^2},\ Nu = \frac{x\ q_{\mathrm{w}}|_{r=R}}{k_f(T_{\mathrm{w}}-T_\infty)},\ Nn = \frac{x\ q_{\mathrm{n}}|_{r=R}}{\widetilde{D}(N_{\mathrm{w}}-N_\infty)} \tag{14}$$

where shear stress, surface heat, and motile surface microorganism fluxes are designated by τ_w, q_n and q_w, the mathematical expressions of which are as follows:

$$\tau_{\mathrm{w}} = \mu_f\frac{\partial u}{\partial r}\left(1+\widetilde{\gamma}^2\left(\frac{\partial u}{\partial r}\right)^2\right)^{(n-1)/2}_{r=R}, q_w = -k_f\left(\frac{\partial T}{\partial r}\right)_{r=R}, q_n = -\widetilde{D}\left(\frac{\partial N}{\partial r}\right)_{r=R} \tag{15}$$

On the basis of the non-similarity transformation (Equation (8)), the obtained non-dimensional mathematical expressions of the skin friction factor C_f, the local Nusselt number Nu, and local density of motile microorganisms Nn can be formulated as follows:

$$\begin{aligned} \mathrm{Re}^{1/2}C_f &= F''(0)\left(1 + W_e F''^2(0)\right)^{(n-1)/2} \\ \mathrm{Re}^{-1/2}Nu &= -\theta'(0) \\ \mathrm{Re}^{-1/2}Nu &= -\vartheta'(0) \end{aligned} \tag{16}$$

in which $\mathrm{Re} = \frac{ax^2}{\nu_f(1-\zeta t)}$ designates the Reynold number.

3. Results and Discussion

In this section, we present an accurate examination of a Carreau two-phase nanofluid flow with swimming gyrotactic microorganisms due to an oblique stretched cylinder under the impact of pertinent factors. The mathematical results are presented as the profiles of the skin-friction factor, heat and mass transmission rates, Carreau temperature, and concentration, which are proven on the basis of Figures 2–13. The MATLAB bvp4c function provides a numerical technique that was employed in order to obtain the solutions of the metamorphic problem equations, i.e., Equations (9)–(12), along with boundary condition equation, Equation (13). The present approach employs the collocation technique in order to solve the boundary value problem in the form

$$y' = F(x, y, P), a \leq x \leq b \tag{17}$$

concerned with general nonlinear, two-point boundary conditions

$$G(y(a), y(b), P) = 0, \tag{18}$$

where p represents a vector of anonymous factors. The approximate solution $H(x)$ indicates a continuous function that is a cubic polynomial on every subinterval x_n, x_{n+1} of a mesh $a = x_0 < x_1 < x_2 < \ldots < x_n = b$, fulfilling the boundary conditions

$$G(H(a), H(b), P) = 0, \tag{19}$$

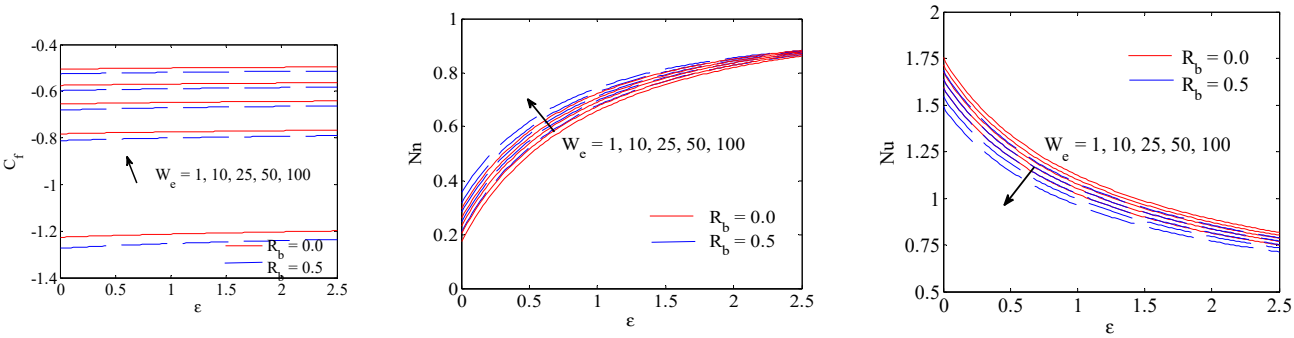

Figure 2. Fluctuations of C_f, Nu and Nn due to W_e factor.

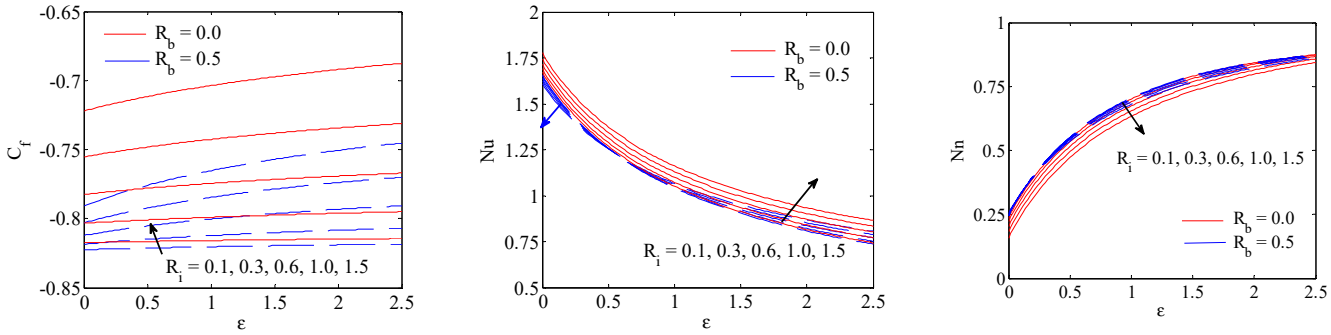

Figure 3. Fluctuations of C_f, Nu and Nn due to R_i factor.

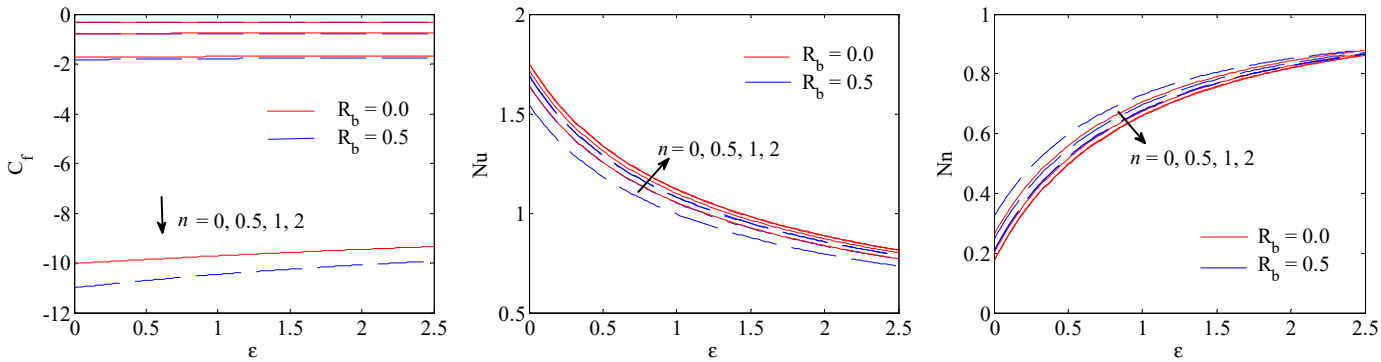

Figure 4. Fluctuations of C_f, Nu and Nn due to n factor.

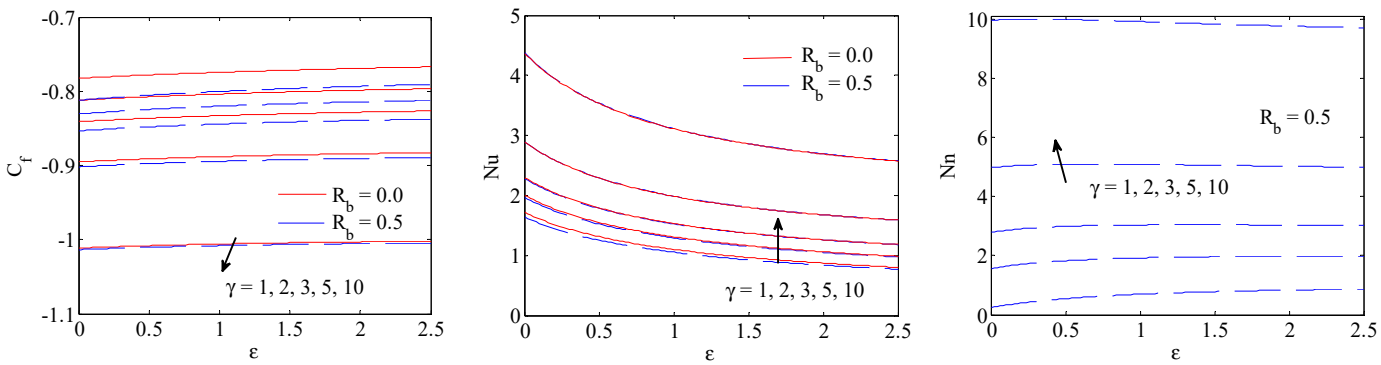

Figure 5. Fluctuations of C_f, Nu and Nn due to γ factor.

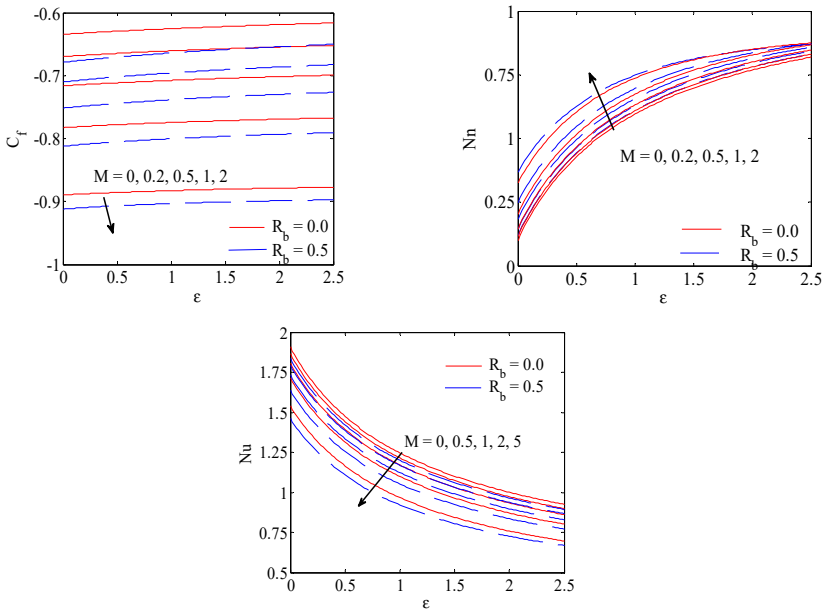

Figure 6. Fluctuations of C_f, Nu and Nn due to the factor M.

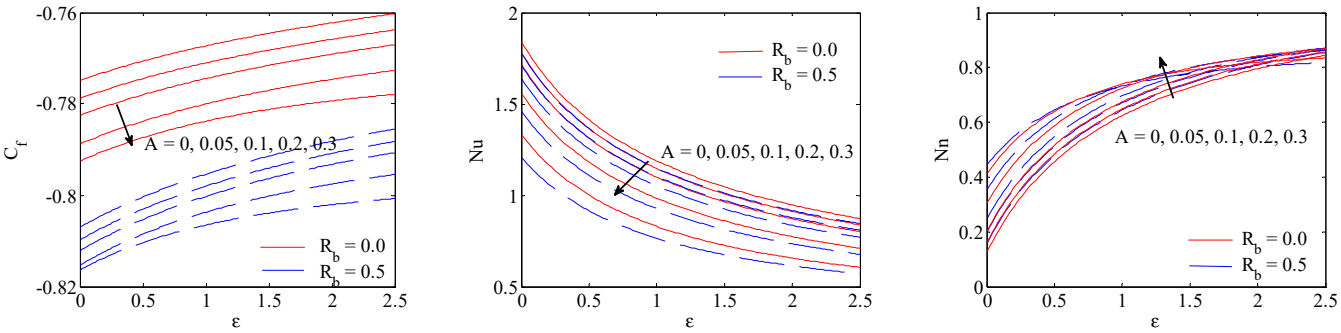

Figure 7. Fluctuations of C_f, Nu and Nn due to the factor A.

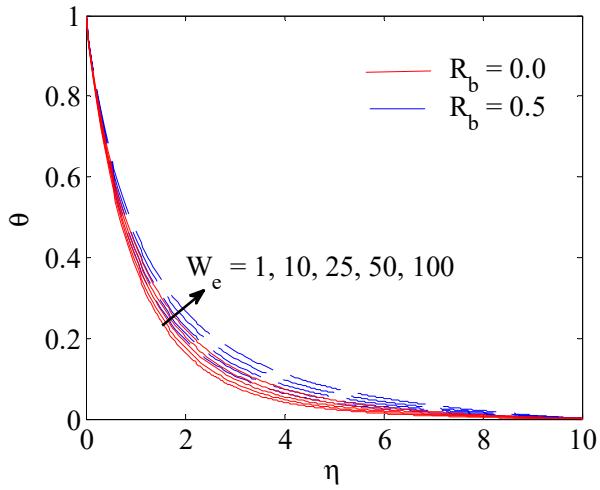

Figure 8. Fluctuations of θ due to the factor W_e.

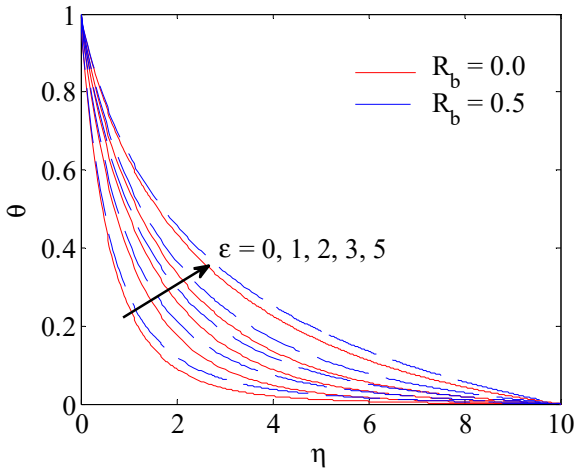

Figure 9. Fluctuations of θ due to the factor ε.

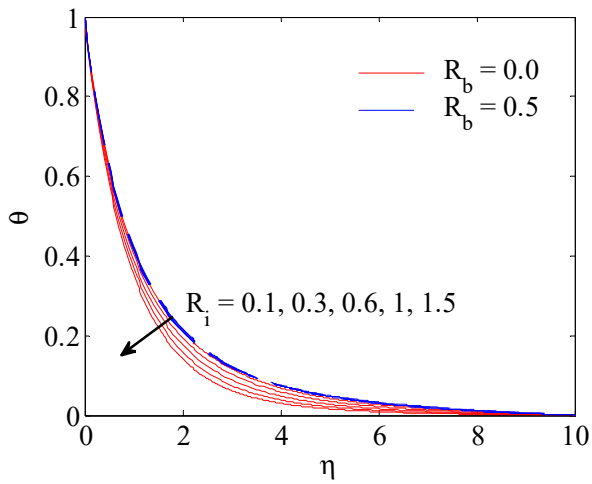

Figure 10. Fluctuations of θ due to the factor R_i.

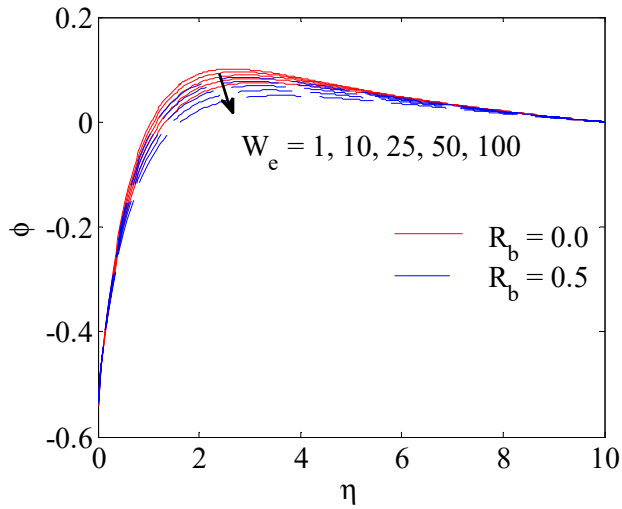

Figure 11. Fluctuations of ϕ due to the factor W_e.

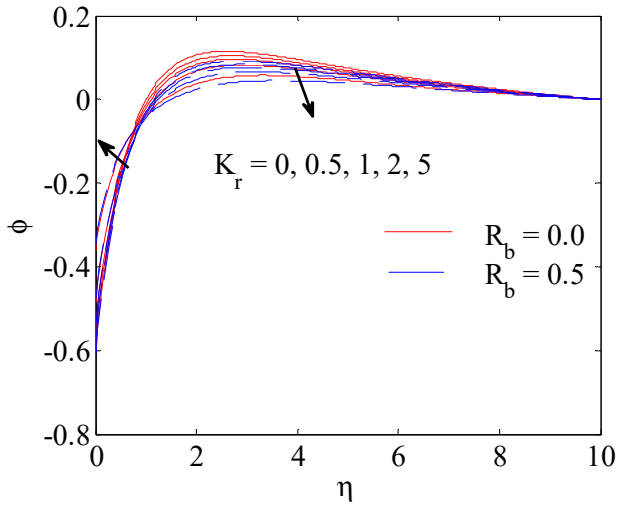

Figure 12. Fluctuations of ϕ due to the factor K_r.

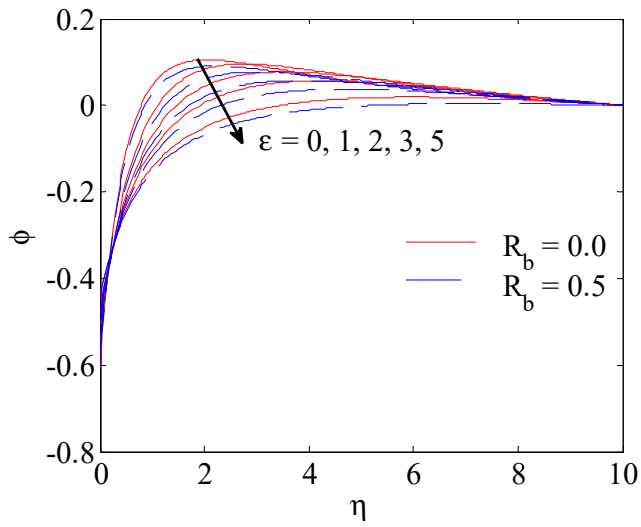

Figure 13. Fluctuations of ϕ due to the factor ε.

This solution also fulfills the set of D.E. at the middle and end points of every subinterval

$$H'(x_n) = F(x_n, H(x_n)), \tag{20}$$

$$H'((x_n + x_{n+1})/2) = F((x_n + x_{n+1})/2, H((x_n + x_{n+1})/2)), \tag{21}$$

$$H'(x_{n+1}) = F(x_{n+1}, H(x_{n+1})) \tag{22}$$

The conditions shown above result in a set of nonlinear algebraic equations for the factors defining H. Furthermore, for confirmation of the method, Table 1 presents a comparison of the data for the skin friction coefficient $\mathrm{Re}^{1/2}\, C_f$ computed for various values of curvature factor (γ) for the particular case of a Newtonian fluid ($n = 1$ or $W_e = 0$) with independent time flow ($A = 0$) and in the absence of magnetic and buoyancy force factors ($B_0 = R_i = 0$); an excellent agreement can be observed with earlier published data by Hashim et al. [45] and Rangi and Ahmad [46]. The range of imposed parameters is $1 \le W_e \le 100$, $0 \le n \le 2$, $0 \le M \le 2$, $0.1 \le R_i \le 1.5$, 0 (no microorganisms) $\le R_b \le 0$, $0 \le \epsilon \le 5.0$, 0 (steady state) $\le A \le 0.3$, $1 \le \gamma \le 10$, and $0 \le K_r \le 5$. The values of the pertinent default factors were given as $W_e = 10$, $m = n = 0.5$, $N_b = N_t = 0.7$, $M = 1$, $R_i = 0.6$, $R_b = 0.0, 0.5$, $P_e = 0.7$, $A = 0.1$, $\mathrm{Pr} = 10$, $\epsilon = 1.0$, $\omega = 0.2$, $L_e = 2$, $L_b = 1.0$, $\gamma = 1.0$, $E = 2.0$, $K_r = 1.0$, $N_r = \delta = 0.5$ unless otherwise stated.

Table 1. A comparison of skin friction $-\mathrm{Re}^{1/2}\, C_f$.

γ	[45]	[46]	Present
0	1.000000	1.000000	1.000000
0.25	1.094373	1.094378	1.094376
0.50	1.188727	1.188715	1.188728
0.75	1.281819	1.281833	1.281827
1.0	1.453373	1.459308	1.453361

Figure 2 presents the fluctuations of the skin friction coefficient $\mathrm{Re}^{1/2}\, C_f$ the Nusselt $\mathrm{Re}^{-1/2}\, Nu$, and density of motile microorganisms $\mathrm{Re}^{-1/2} Nn$ associated with thermal conductivity factor ϵ as a function of W_e factor, where $W_e = 1, 10, 25, 50, 100$. Weissenberg number is defined in terms of specific process time and relaxation time, and, with increasing values of relaxation time yields increased resistance between fluid particles, that is, higher Weissenberg numbers result in increased viscosity in the Carreau nanofluid, and thus, the flow fluctuation of the fluid presents a decreasing trend. The plotted outcomes presented in this figure indicate that as the Weissenberg number W_e increases, the magnitude of both skin friction coefficient and Nusselt number decrease, while the value of the local density of motile microorganisms increases. Additionally, it is obvious that the magnitude of skin friction is weaker in the case of flow over a stretching cylinder without microorganisms. The changes in the values of skin friction coefficient, rate of heat transmission, and density of motile microorganisms for miscellaneous values of buoyancy ratio factor (R_i = 0.1, 0.3, 0.6, 1.0, 1.5) under cases $R_b = 0$ and 0.5 are presented in Figure 3.

It can be seen that the magnitude of the skin friction coefficient and the density of motile microorganisms decreases with increasing buoyancy ratio factor, whereas the rate of heat transmission expressed in terms of Nusselt number increases. Since the buoyancy force has a dominant impact on viscous forces for larger values of R_i, the mixed convection factor is responsible for making the fluid flow faster, which is undertaken with the aim of improving the motion of the fluid.

The impact of the power-law index factor n, where $n = 0, 0.5, 1, 2$, on skin friction, Nusselt number, and density of motile microorganisms is presented in Figure 4, with $\mathrm{R_b} = 0, 0.5$. Please note that, physically, the power-law index n describes the slope $(\mu - \mu_\infty)/(\mu_0 - \mu_\infty)$ in the power-law region. As can be seen, both theabsolute value of skin friction and the gradient of temperature improve with increasing values of the factor n, but the opposite trend is observed for the density of motile microorganisms. Physically, an improvement in the Carreau fluid factor n enhances the viscosity of the fluid, resulting in a weakened opposing force.

It is well known that the curvature factor corresponds inversely with the radius of a cylinder, and thus an increment in curvature will lead to a decrease in the cylinder area, and consequently reduced contact between the fluid elements and the cylinder, as well as a subsequent reduction intemperature as a consequence of the reduction in the surface domain of cylinder in contact with the fluid. The impact of curvature factor γ is presented in Figure 5 for the cases with both thepresence andabsence of microorganisms. From the figure, it is clear that the factor γ increases the values of skin friction, Nusselt number, and density of motile microorganisms.

Figure 6 illustrates the trends of C_f, Nu and Nn with respect to thermal conductivity factor ϵ for miscellaneous magnetic field factor M. The magnetic field factor indicates the ratio of magnetic force to viscous force, such that increasing values of M explicitly enhance Lorentz force (anti-flow force). This drag-like force induces greaterresistance to transport phenomena due to the decrease in movement and increases the thickness ofthe thermal boundary layer. As can be seen, negative values of dragforce and density of motile microorganisms are improved, but the Nusselt number decreases. Negative values of C_f and Nn are found to exhibit an increasing trend when investigating the unsteadiness factor A bothwith andwithout microorganisms, whereas increasing A causes a decrease inthe Nusselt number, as shown in Figure 7.

It is clear that when unsteadiness increases, the cylinder surface loses more heat. Additionally, temperature variations in the non-Newtonian Carreau nanofluid are presented in Figure 8 with a variety of values of Weissenberg number W_e. Our observations reveal that increasing values of W_e boost the nanofluid temperature through the boundary layer both with and without the presence of microorganisms. The impactof non-uniform thermal conductivity factor ϵ (varying from 0 to 5) on temperature distribution is presented in Figure 9. It can be seen that as the particles collide with each other, they transmit energy, which causes increased temperature distribution. As a result, increases in the thermal conductivity factor yield augmentation in the temperature of the Carreau nanofluid. Therefore, the trend of temperature is an ascending state with increasing values of ϵ.

As can be clearly seen in Figure 10, the mixed convection factor R_i results in decreased Careau nanofluid temperature profiles. The influencesof theWeissenberg number, chemical reaction, and non-uniform thermal conductivity factors on variations in microorganism concentration are shown in Figures 11–13. As can be seen, all W_e, K_r and ϵ factors present a decrease in the profile of microorganism concentration. It isclear that an increasing reaction rate constant yields an augmentation in the term $(1+\delta\theta)^m EXP\left(\frac{-E}{1+\delta\theta}\right)$. This leads to the occurrence of a destructive chemical reaction, as well as a subsidence in the mass fraction profile.

4. Conclusions

The key aim of the present analysis was to scrutinize the trend of swimming motile microorganisms in a time-dependent MHD 2-D convectional flow of Carreau nanomaterials around an oblique cylinder. The novel notions of non-uniform thermal conductivity and variable magnetic field were employed in order to consider the flow problem. The conclusions drawn from the investigation are briefly presented as follows:

- The absolute drag force increases with increasing curvature, unsteadiness, magnetic field and power-law factors, while it decreases with increasing Weissenberg number and mixed convection factor.
- For shear-thinning fluid, a substantial decrease in the velocity and momentum boundary layer thickness is noticed with increasing Weissenberg number.
- The temperatures curves increase with incrementation of both Weissenberg number and non-uniform thermal conductivity factor, but decrease due to mixed convection.
- The solutal fluctuations decrease with increasing values of Weissenberg number, as well as non-uniform thermal conductivity and chemical reaction factors.
- Absolute drag force and local values of density of motile microorganisms increase due to A and M factors, while the local Nusselt number decreases.
- The heat transmission rate over the surface is greater for a cylinder than for a flat surface.
- The local Nusselt number in shear-thinning fluid decreases with incrementation of the W_e number.
- Mixed convection and power-law factors result in increased magnitude of drag force and Nusselt number, but decreased density of motile microorganisms.

Author Contributions: All authors contributed to this work equally. All authors have read and agreed to the published version of the manuscript.

Funding: The authors extend their appreciation to the Deputyship for Research & Innovation, Ministry of Education in Saudi Arabia, for funding this research work through the project number (IF-PSAU-2021/01/17862).

Institutional Review Board Statement: Not applicable.

Informed Consent Statement: Not applicable.

Data Availability Statement: Data available upon request.

Conflicts of Interest: The authors declare no conflict of interest.

References

1. Careau, P.J. Rheological equations from molecular network theories. *Trans. Soc. Rheol.* **1972**, *116*, 99–127. [CrossRef]
2. Chhabra, R.P.; Uhlherr, P.H.T. Creeping motion of spheres through shear-thinning elastic fluids described by the Carreau viscosity equation. *Rheol. Acta* **1980**, *19*, 187–195. [CrossRef]
3. Tang, H.; Kefayati, G. Double-diffusive laminar natural convection and entropy generation of Carreau fluid in a heated enclosure with an inner circular cold cylinder (Part II: Entropy generation). *Int. J. Heat Mass Transf.* **2018**, *120*, 683–713.
4. Sochi, T. Analytical solutions for the flow of Carreau and Cross fluids in circular pipes and thin slits. *Rheol. Acta* **2015**, *54*, 745–756. [CrossRef]
5. Griffiths, P.T. Flow of a generalized Newtonian fluid due to a rotating disk. *J. Non-Newton. Fluid Mech.* **2015**, *221*, 9–17. [CrossRef]
6. Liron, N.; Wilhelm, H. Integration of magnetohydrodynamic boundary layer equation. *Appl. Math. Mech. ZAMM* **1974**, *54*, 27–37. [CrossRef]
7. Soomro, F.A.; Usman, M.; Haq, R.U.; Wang, W. Thermal and velocity slip effects on MHD mixed convection flow of Williamson nanofluid along a vertical surface: Modified Legendre wavelets approach, Physica E: Low-dim. *Syst. Nanostruct.* **2018**, *104*, 130–137. [CrossRef]
8. Pal, D.; Mandal, G.; Vajravelu, K. MHD convection–dissipation heat transfer over a non-linear stretching and shrinking sheets in nanofluids with thermal radiation. *Int. J. Heat Mass Transf.* **2013**, *65*, 481–490. [CrossRef]
9. Daniel, Y.S.; Aziz, Z.A.; Ismail, Z.; Salah, F. Double stratification effects on unsteady electrical MHD mixed convection flow of nanofluid with viscous dissipation and Joule heating. *J. Appl. Res. Technol.* **2017**, *15*, 464–476. [CrossRef]
10. Shankaralingappa, B.M.; Madhukesh, J.K.; Sarris, I.E.; Gireesha, B.J.; Prasannakumara, B.C. Influence of Thermophoretic Particle Deposition on the 3D Flow of Sodium Alginate-Based Casson Nanofluid over a Stretching Sheet. *Micromachines* **2021**, *12*, 1474. [CrossRef]
11. Shankaralingappa, B.M.; Prasannakumara, B.C.; Gireesha, B.J.; Sarris, I.E. The impact of Cattaneo–Christov double diffusion on Oldroyd-B Fluid flow over a stretching sheet with thermophoretic particle deposition and relaxation chemical reaction. *Inventions* **2021**, *6*, 95. [CrossRef]
12. Khan, M.; Hashim. Boundary layer flow and heat transfer to Carreau fluid over a nonlinear stretching sheet. *AIP Adv.* **2015**, *5*, 107203. [CrossRef]
13. Khan, M.; Hashim. Axisymmetric flow and heat transfer of the Carreau fluid due to a radially stretching sheet: Numerical study. *J. Appl. Mech. Tech. Phys.* **2017**, *58*, 410–418. [CrossRef]
14. Animasaun, I.; Pop, I. Numerical exploration of a non-Newtonian Carreau fluid flow driven by catalytic surface reactions on an upper horizontal surface of a paraboloid of revolution, buoyancy and stretching at the free stream. *Alex. Eng. J.* **2017**, *56*, 647–658. [CrossRef]
15. Akbar, N.S.; Nadeem, S.; Khan, Z.H. Numerical simulation of peristaltic flow of a Carreau nanofluid in an asymmetric channel. *Alex. Eng. J.* **2014**, *53*, 191–197. [CrossRef]
16. Makinde, O.D.; Kumara, B.P.; Ramesh, G.; Gireesha, B.J. Simultaneous Convection of Carreau Fluid with Radiation Past a Convectively Heated Moving Plate. *Defect Diffus. Forum* **2018**, *389*, 60–70. [CrossRef]
17. Muhammad, T.; Alamri, S.Z.; Waqas, H.; Habib, D.; Ellahi, R. Bioconvection flow of magnetized Carreau nanofluid under the influence of slip over a wedge with motile microorganisms. *J. Therm. Anal.* **2021**, *143*, 945–957. [CrossRef]
18. Mahdy, A.; Hady, F.M.; Mohamed, R.A.; Abo-Zaid, O.A. Activation energy effectiveness in dusty Carreau fluid flow along a stretched cylinder due to nonuniform thermal conductivity property and temperature-dependent heat source/sink. *Heat Transf.* **2021**, *50*, 5760–5778. [CrossRef]
19. Pantokratoras, A. Non-similar Blasius and Sakiadis flow of a non-Newtonian Carreau fluid. *J. Taiwan Inst. Chem. Eng.* **2015**, *56*, 1–5. [CrossRef]
20. Khan, M.I.; Haq, F.; Hayat, T.; Alsaedi, A.; Rahman, M.U. Natural bio-convective flow of Sisko nanofluid subject to gyrotactic microorganisms and activation energy. *Phys. Scr.* **2019**, *94*, 125203. [CrossRef]
21. Waqas, H.; Khan, S.U.; Hassan, M.; Bhatti, M.; Imran, M. Analysis on the bioconvection flow of modified second-grade nanofluid containing gyrotactic microorganisms and nanoparticles. *J. Mol. Liq.* **2019**, *291*, 111231. [CrossRef]
22. Shen, B.; Zheng, L.; Zhang, C.; Zhang, X. Bioconvection heat transfer of a nanofluid over a stretching sheet with velocity slip and temperature jump. *Therm. Sci.* **2017**, *21*, 2347–2356. [CrossRef]
23. Balla, C.S.; Haritha, C.; Naikoti, K.; Rashad, A.M. Bioconvection in nanofluid saturated porous square cavity containing oxytactic microorganisms. *Int. J. Numer. Methods Heat Fluid Flow* **2019**, *29*, 1448–1465. [CrossRef]
24. Ramzan, M.; Mohammad, M.; Howari, F. Magnetized suspended carbon nanotubes based nanofluid flow with bio-convection and entropy generation past a vertical cone. *Sci. Rep.* **2019**, *9*, 12225. [CrossRef] [PubMed]
25. Mahdy, A. Natural convection boundary layer flow due to gyrotactic mico-organisms about a vertical cone in porous media saturated by a nanofluid. *J. Braz. Soc. Mech. Sci. Eng.* **2016**, *38*, 67–76. [CrossRef]
26. Mahdy, A.; Nabwey, H.A. Microorganisms time-mixed convection nanofluid flow by the stagnation domain of an impulsively rotating sphere due to Newtonian heating. *Results Phys.* **2020**, *19*, 103347. [CrossRef]
27. Ahmed, S.E.; Mahdy, A. Laminar MHD natural convection of nanofluid containing gyrotactic microorganisms over vertical wavy surface saturated non-Darcian porous media. *Appl. Math. Mech.* **2016**, *37*, 471–484. [CrossRef]

28. Zeeshan, A.; Ali, Z.; Gorjiy, M.R.; Hussain, F.; Nadeem, S. Flow analysis of bioconvection heat and mass transfer of two-dimensional couple stress fluid over a paraboloid of revolution. *Int. J. Mod. Phys. B* **2020**, *34*, 2050110. [CrossRef]
29. Biswas, N.; Manna, N.K.; Mandal, D.K.; Gorla, R.S.R. Magnetohydrodynamic mixed bioconvection of oxytactic microorganisms in a nanofluid-saturated porous cavity heated with a bell-shaped curved bottom. *Int. J. Numer. Methods Heat Fluid Flow* **2021**, *31*, 3722–3751. [CrossRef]
30. Mahdy, A. Unsteady Mixed Bioconvection Flow of Eyring–Powell Nanofluid with Motile Gyrotactic Microorganisms Past Stretching Surface. *BioNanoScience* **2021**, *11*, 295–305. [CrossRef]
31. Uddin, J.; Kabir, M.N.; Bég, O.A. Computational investigation of Stefan blowing and multiple-slip effects on buoyancy-driven bioconvection nanofluid flow with microorganisms. *Int. J. Heat Mass Transf.* **2016**, *95*, 116–130.
32. Naseem, F.; Shafiq, A.; Zhao, L.; Naseem, A. MHD biconvective flow of Powell Eyring nanofluid over stretched surface. *AIP Adv.* **2017**, *7*, 065013. [CrossRef]
33. Tham, L.; Nazar, R.; Pop, I. Mixed convection flow over a solid sphere embedded in a porous medium filled by a nanofluid containing gyrotactic microorganisms. *Int. J. Heat Mass Transf.* **2013**, *62*, 647–660. [CrossRef]
34. Choi, S. Enhancing thermal conductivity of fluids with nanoparticle. In *Developments and Applications of Non-Newtonian Flows*; Siginer, D.A., Wang, H.P., Eds.; Argonne National Lab (ANL): Argonne, IL, USA, 1995; pp. 99–105.
35. Buongiorno, J. Convective Transport in Nanofluids. *J. Heat Transfer* **2006**, *128*, 240–250. [CrossRef]
36. Yusuf, T.; Mabood, F.; Prasannakumara, B.; Sarris, I. Magneto-Bioconvection Flow of Williamson Nanofluid over an Inclined Plate with Gyrotactic Microorganisms and Entropy Generation. *Fluids* **2021**, *6*, 109. [CrossRef]
37. Majeed, A.; Zeeshan, A.; Noori, F.M. Numerical study of Darcy—Forchheimer model with activation energy subject to chemically reactive species and momentum slip of order two. *AIP Adv.* **2019**, *9*, 045035.
38. Khan, M.I.; Hayat, T.; Alsaedi, A. Activation energy impact in nonlinear radiative stagnation point flow of Cross nanofluid. *Int. Commun. Heat Mass Transf.* **2018**, *91*, 216–224. [CrossRef]
39. Mustafa, M.; Khan, J.A.; Hayat, T.; Alsaedi, A. Buoyancy effects on the MHD nanofluid flow past a vertical surface with chemical reaction and activation energy. *Int. J. Heat Mass Transf.* **2017**, *108*, 1340–1346. [CrossRef]
40. Dhlamini, M.; Kameswaran, P.K.; Sibanda, P.; Motsa, S.; Mondal, H. Activation energy and binary chemical reaction effects in mixed convective nanofluid flow with convective boundary conditions. *J. Comput. Des. Eng.* **2019**, *6*, 149–158. [CrossRef]
41. Shafique, Z.; Mustafa, M.; Mushtaq, A. Boundary layer flow of Maxwell fluid in rotating frame with binary chemical reaction and activation energy. *Results Phys.* **2016**, *6*, 627–633. [CrossRef]
42. Zhao, Q.; Xu, H.; Tao, L. Flow and heat transfer of nanofluid through a horizontal microchannel with magnetic field and interfacial electrokinetic effects. *Eur. J. Mech. B Fluids* **2020**, *80*, 72–79. [CrossRef]
43. Waqas, M.; Farooq, M.; Khan, M.I.; Alsaedi, A. Magnethydrodynamic (MHD) mixed convection flow of micropolar liquid due to nonlinear stretched sheet with convective condition. *Int. J. Heat Mass Transf.* **2016**, *102*, 766–772. [CrossRef]
44. Kumar, R.K.; Varma, S. MHD Boundary Layer Flow of Nanofluid Through a Porous Medium Over a Stretching Sheet with Variable Wall Thickness: Using Cattaneo–Christov Heat Flux Model. *J. Theor. Appl. Mech.* **2018**, *48*, 72–92. [CrossRef]
45. Hashim; Khan, M.; Alshomrani, A.S. Characteristics of melting heat transfer during flow of Carreau fluid induced by a stretching cylinder. *Eur. Phys. J. E* **2017**, *40*, 8. [CrossRef]
46. Rangi, R.R.; Ahmad, N. Boundary Layer Flow past a Stretching Cylinder and Heat Transfer with Variable Thermal Conductivity. *Appl. Math.* **2012**, *3*, 205–209. [CrossRef]